British Journal of Pharmacology (2001) 132, 63–72

www.nature.com/bjp

Novel mechanism of blocking axonal Na^+ channels by three macrocyclic polyamine analogues and two spider toxins

[1,4]Masuhide Yakehiro, [1,5]Yasuo Furukawa, [2]Tohru Koike, [2]Eiichi Kimura, [3,6]Terumi Nakajima, [1]Kaoru Yamaoka & *,[1]Issei Seyama

[1]Department of Physiology, School of Medicine, Hiroshima University, Hiroshima 734-8551, Japan; [2]Institute of Pharmaceutical Sciences, Hiroshima University, Hiroshima 734-8551, Japan and [3]Department of Pharmaceutical Sciences, Tokyo University, Tokyo 113-0033, Japan

1 The mechanism of Na^+ channel block by three macrocyclic polyamine derivatives and two spider toxins was studied with voltage clamp and internal perfusion method in squid axons.

2 All these chemicals specifically block Na^+ channels in the open state only from the internal surface, and do not affect K^+ channels.

3 The blocking effect is enhanced as the depolarizing pulse becomes larger. Blocked channels are unable to shift to the inactivated state.

4 In the case of cyclam and guanidyl-side armed cyclam (G-cyclam), quick release of these chemicals from the binding sites is proven by the increase in the tail current and prolongation of the time course of the off gating current. On the other hand, in the presence of N-4 and the spider toxins, their detachment was delayed significantly.

5 Molecular requirements for the block of Na^+ channels by these molecules are the presence of positive charge and hydrophobicity.

British Journal of Pharmacology (2001) **132,** 63–72

Keywords: JSTX-3; NSTX-3; macrocyclic polyamine; Na^+ channel; block; internal phase; spider toxin

Abbreviations: cyclam, 1,4,8,11-tetra-azacyclotetradecane; DAAC, 2,4-dihydroxyphenylacethylasparaginyl cadaverine group; G-cyclam, guanidyl-side armed cyclam; h_∞ curve, steady-state inactivation curve; I_{Na}, Na current; I–V relation, current-voltage relation; K_D, dissociation constant

Introduction

Na^+ channels are regulated both by activation and inactivation gating mechanisms. During the gating process, Na^+ channels become briefly permeable to sodium ions, leading to the generation of action potentials. These complex functional properties of Na^+ channel proteins can be related to conformational changes. Since the pioneering work begun by the late Numa's group to determine the primary structure of Na^+ channel in *Electrophorus electricus* (Noda *et al*., 1984), many models of the putative Na^+ channel structure have been put forward. However, understanding Na^+ channel function on structural basis is unlikely in the foreseeable future because proteins are difficult to crystallize when embedded in a lipid bilayer. At present we can obtain insight from the deduced amino acid sequences, the effects of specific mutants and the availability of specific pharmacological probes.

Valuable tools for the investigation of the functional structure of Na^+ channel are natural toxins and chemicals, which have high affinity and blocking efficacy and which interact specifically with Na^+ channels. Some of the most successful examples of small natural toxins are tetorodotoxin (TTX) and saxitoxin; they have been used to attempt to define the shape and structure of the outer vestibule of Na^+ channels. Availability of these natural toxins allows us to infer the size of outside vestibule and the distribution of negative charges around ion sieving structures (Fozzard & Hanck, 1996). Another example of toxins that yield structural information is sea anemone toxin and α-scorpion toxin, which interfere with the inactivation process of Na^+ channels. Their binding to the loop between segment 3 and segment 4 in domain IV in Na^+ channels appears to be critical for this process (Rogers *et al*., 1996).

So far, information on the functional structure of Na^+ channels is limited to the extracellular vestibule. In order to obtain more precise insight into the structure for the intracellular side of Na^+ channel, it is highly desirable that more natural toxins and chemicals, which exclusively affect the Na^+ channel function from the internal phase, are available. In this study, we added three new cyclic polyamine derivatives and two spider toxins to the list of molecules, such as pancuronium (Yeh & Narahashi, 1977), N-methylstrychinine (Cahalan & Almers, 1979) and Azure A (Armstrong & Croop, 1982), which block Na^+ channel only from the internal phase. Cyclic polyamine derivatives (G-cyclam, cyclam and N-4) bear a cyclic tetraamine structure in common. Furthermore, it is reasonable to speculate that both JSTX-3 and NSTX-3 are in a configuration similar to cyclic polyamine, because the spider toxins have been considered to

*Author for correspondence.
Current addresses: [4]Division of Physiology, Department of Clinical Engineering, Hiroshima International University, Faculty of Health Sciences, 555-36 Gakuendai, Kurose-cho, Kamo-gun, Hiroshima Prefecture, 732-0695, Japan; [5]Department of Biological Science, Faculty of Science, Hiroshima University, Kagamiyama 1-3-1, Higashihiroshima 739-8526, Japan; [6]Suntry Institute for Bioorganic Research, Shimamoto-cho, Mishima-gun, Osaka, 618-8503 Japan

make a compact ring configuration in aqueous environment by the Zn^{2+} complexation (Kawai *et al*., 1989) or intramolecular hydrogen bonding. So all the chemicals used in this study are considered to be variations of cyclam, to which positive charges or hydrophobicity are added. Therefore, we could systematically test the effectiveness of charges and hydrophobicity in blocking action, leading to a precise understanding of chemical characteristics playing an important role in blocking Na^+ channels in axons.

Methods

All experiments were performed on cleaned, internally perfused axons of *Doryteuthis bleekeri* and *D. kensaki*. The method employed for the internal perfusion was similar to that of Narahashi & Anderson (1967). The electrode and the voltage clamp method were essentially the same as those described previously (Wu & Narahashi, 1973), with the exception that the series resistance compensation was incorporated in the voltage clamp circuit. The series resistance was determined by measurement of a potential jump caused by a brief current step, and was partially compensated for as described by Armstrong (1969). Junction potentials were corrected for in the internal perfused axons.

The axons were perfused and voltage clamped by standard methods and the membrane currents were recorded on magnetic disk for later analysis. When necessary, the axons were perfused with pronase-containing internal solutions (1 mg ml^{-1}) for 1–10 min to remove the sodium channel inactivation. The solutions used are listed in Table 1 together with their compositions. The combination of perfusates is presented in external perfusate/internal perfusate (in abbreviated form). All experiments were carried out at 6°C. Data are presented as mean ± standard deviation of mean (n = number of observations), unless otherwise stated. Statistical significance was tested by the Student's t-test.

G-cyclam was synthesized from 6-(4-aminobuthyl)-1,4,8,11-tetraazacyclotetradecane (amino-pendant cyclam). A solution of amino-pendant cyclam (540 mg, 2.0 mol) and *S*-methylisothiourea sulphate (560 mg, 2.0 mol) in 10 ml of H_2O was heated at 50°C for 1 day. After evaporating the solvent, the solid residue was recrystallized from 6 M HBr aqueous solution to give 6-(4-guanidinobuthyl)-1,4,8,11-tetraazacyclotetradecane as pentahydrobromide ($1{\cdot}5\ HBr \cdot 1.5\ H_2O$, 800 mg, 54% yield). Its chemical structure was confirmed by ^{1}H-NMR, IR spectroscopy and elementary analysis. Cyclam was purchased from Aldrich Chemical Co. (WI, U.S.A.). JSTX-3 and NSTX-3 were isolated and purified, as described previously (Aramaki *et al*., 1986). The polyamine parts extended from 2,4-dihydroxyphenylacetylasparaginylcadaverino-moiety in JSTX-3 and NSTX-3 have been shown to be semicircular in configuration in aqueous solution by the two-dimensional NMR method, suggesting that the physical size of spider toxins is not much different from that of polyamine analogues. The synthetic method for N4 has been described elsewhere (Kawai *et al*., 1989). The molecular structure of the five molecules is presented in Figure 1. All the pharmacological agents were diluted directly into the experimental solutions, or were prepared as stock solutions in distilled deionized water and were diluted into the desired media immediately before use.

Results

Suppression of I_{Na}

Figure 2A,B illustrate how intracellularly applied 0.1 mM G-cyclam affected the membrane currents in intact axons. Conspicuous suppression was recognized only during the flow of Na^+ current (I_{Na}), in which the decay of I_{Na} is accelerated. The resultant current-voltage relations (I–V relation) are presented in Figure 2D, and suggest that the more the membrane was depolarized, the more significantly I_{Na} decreased. Suppression of steady state currents became apparent only at the range of extremely depolarized membrane potential. The effect of G-cyclam was reversible (data not shown).

To ascertain the time course of Na^+ channel block with G-cyclam, we carried out a similar experiment on axons with Cs^+ internal solution. Conspicuous suppression of peak I_{Na},

Table 1 Compositions of external and internal solutions (mM)

	External solutions				*Internal solutions*		
	ASW	*450 Na^+-ASW*	*50 Na^+-ASW*	*Na^+-free ASW**	*SIS*	*50 Na^+-SIS*	*Na^+-free SIS*
NaCl	450	450	50				
TMA-Cl‡			400	450			
KCl	10						
$CaCl_2 2H_2O$	50	50	50	50			
TRIS§	30	10	10	10			
HEPES**		10	10	10		10	10
NaF					50	8.3	
NaOH						41.7	
CsF						41.7	50
CsOH						208.3	250
L-glutamic acid (monopotassium salt)					320		
L-glutamic acid						250	250
K-phosphate buffer#					15		
Sucrose					333	500	500

*1 μM tetrodotoxin is added. ‡tetramethylammonium chloride. §tris(hydroxymethyl)aminomethane. **N-2-hydroxyethylpiperazine-N′-2-ethanesulphonic acid. #KH_2PO_4-KOH buffer pH 7.65. The external solutions were titrated to pH 8.0 with HCl, and the internal solutions to pH 7.3 with L-glutamic acid or CsOH (KOH for SIS).

as well as a faster decline of I_{Na}, was observed (Figure 2C). Another noteworthy point is that G-cyclam not only increased the amplitude of I_{Na} tail current but also prolonged its time course (shown in Figure 2C). All other molecules studied exerted a qualitatively similar suppressive action on I_{Na} ($n=4$ for 0.3 mM cyclam and $n=3$ for 0.1 mM N4 and two spider toxins; data not shown). External application of G-cyclam and cyclam and two spider toxins, at the same concentration as in the internal application, did not change I_{Na}.

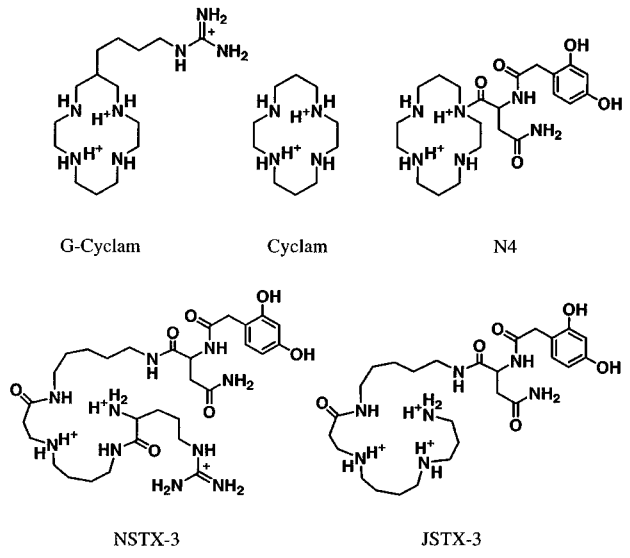

Figure 1 Chemical structure of macrocyclic polyamine analogues and spider toxins tested.

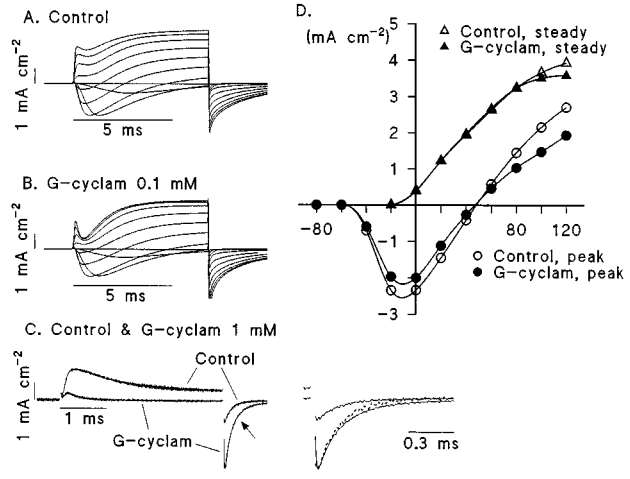

Figure 2 Effects of internal application of G-cyclam on the membrane currents in squid axon. (A) Families of currents in control in response to a series of depolarizations from −60 to +120 mV in 20 mV steps in ASW/SIS medium. (B) Those in 0.1 mM G-cyclam. (C) Enhancement and prolongation of tail current of I_{Na} by G-cyclam. A striking increase in the tail current (shown by arrow), as well as suppression of I_{Na}, appeared with the application of 1 mM G-cyclam when the membrane depolarized to +120 mV from a holding potential of −80 mV. In inset figure, to ascertain the prolongation of tail current in G-cyclam, tail current in control (in dotted line) was scaled to match its peak with that in G-cyclam. The record was taken in 450 Na^+-ASW/50 Na^+-SIS. (D) Current-voltage relationship.

Since I_{Na}, especially in the depolarized membrane potential range, keeps flowing at the end of a 7 ms pulse (Chandler & Meves, 1970) (also referred to in Figure 2C), we needed to study the action of macrocyclic polyamines and two spider toxins on K^+ current (I_K) after complete elimination of I_{Na} by 1 μM external TTX. In this condition, we failed to see any change in I_K ($n=3$ for 1 mM G-cyclam and cyclam and $n=2$ for 0.3 mM N4 and two spider toxins; data not shown).

Effect on steady-state inactivation curves (h_∞ curves)

Steady-state inactivation curves were obtained by a conventional method in which the conditioning pulses of various amplitudes for 50 ms are followed by a constant test pulse to 0 mV (Figure 3). A gap between the conditioning and test pulses was deliberately not introduced in order to eliminate a possible recovery of the drug-binding from Na^+ channels. We applied a Boltzmann formalism to the data generated with below 0 mV. V_h, the membrane potential at which half inactivation occurs and the slope factor, k, were calculated to be -42.1 ± 3.2 mV and 14.3 ± 3.8 mV ($n=4$) in control solutions. These values were -42.7 ± 2.1 mV and 13.3 ± 2.2 mV ($n=4$) in G-cyclam, and, for cyclam, -37.5 ± 3.2 mV and 12.7 ± 1.1 mV ($n=4$) in control, and -42.7 ± 3.0 mV and 15.3 ± 3.5 mV in cyclam, respectively. Because the supply of N-4 and the two spider toxins was limited, only two experiments were performed on each of them. Qualitatively similar data were obtained (data not shown). Previously it has been observed that beyond 0 mV, inactivation occurs incompletely in perfused squid axon (Chandler & Meves, 1970). In the presence of all the

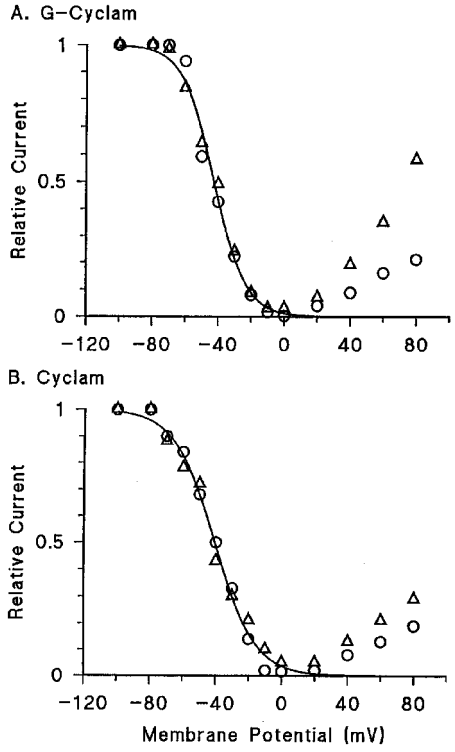

Figure 3 Effect of internal application of G-cyclam and cyclam on the steady-state inactivation curve for Na^+ channels in intact axon in 450 Na^+-ASW/50 Na^+-SIS medium.

compounds tested, the extent of incompleteness in h_∞ curve is more prominent as the conditioning pulse becomes higher. This curious behaviour of h_∞ curve can be explained by the voltage-dependent block of Na^+ channels (discussed below).

Kinetic analysis of the suppression of I_{Na}

It is difficult to study the mode of suppression of I_{Na} on intact axons because the time course of the blocking of Na^+ channels by means of these compounds overlaps with that of the inactivation process. To eliminate this difficulty, we carried out experiments on pronase-treated axons, in which the Na^+ channels remain open upon depolarization and stay open for seconds (Rojas & Rudy, 1976). An example of the interaction of G-cyclam with open sodium channel is illustrated in Figure 4. In pronase-treated axons, step depolarization to +120 mV induces a quick increase in Na^+ conductance in the initial stage in macrocyclic polyamine medium similar to that in the drug free medium, implying that these compounds bind after Na^+ channels open. For this reason, blocking effect of these compounds became apparent only at a late rising of Na conductance, as peak I_{Na} was suppressed significantly in the drug-containing medium.

Kinetic analysis of the block for pronase-treated axon was carried out under the assumption that drug blocks Na^+ channels only in an open state and that the drug-bound channel is incapable of being closed either by inactivation or by deactivation. Justification for this assumption will be provided below. Another assumption is that drug binds with Na^+ channels on one-to-one basis. This assumption will be justified by the fit of the line of one-to-one stoichiometry to the concentration-response curves (Figure 8).

Because Na^+ channels are blocked in a double exponential time course, two blocked states in a series are assumed to occur.

$$\text{Closed} \rightleftharpoons \text{Open} \underset{l_1}{\overset{k_1}{\rightleftharpoons}} \text{Blocked}_1 \underset{l_2}{\overset{b_2}{\rightleftharpoons}} \text{Blocked}_2$$

Drug binding occurs at $k_1 = b_1 \cdot [\text{drug}]$ where b_1 denotes the constant, and [drug] the drug concentration in M. Calculated values for the four rate constants for G-cyclam and N4 were plotted against the membrane potentials of test pulse (Figures 4 and 6). However, in the cases of cyclam (Figure 5), JSTX-3 and NSTX-3 (data not shown for both cases), the block proceeded in a single exponential function, and calculated values for b (k_1) and 1 (11), assuming $b_2 = 0$, were plotted in Figures 5 and 7.

Dose-response curve for these macrocyclic polyamine analogues

In pronase-treated axons, suppressive effect of the drugs on I_{Na} was quantified by measuring difference current at the end of a 14 ms pulse to +120 mV in the presence and absence of drugs. Relative inhibition of I_{Na} for each concentration of drugs was calculated by dividing the amount of suppression of I_{Na} by the steady state I_{Na} in control. Resultant relative values from +120 mV were plotted against concentrations of drug (Figure 8A-1, B-1 and C-1). Assuming one-to-one stoichiometry, the concentration at which half maximal suppression of I_{Na} (K_D) occurred is estimated. Using the same procedure, K_D for each testing potential was determined

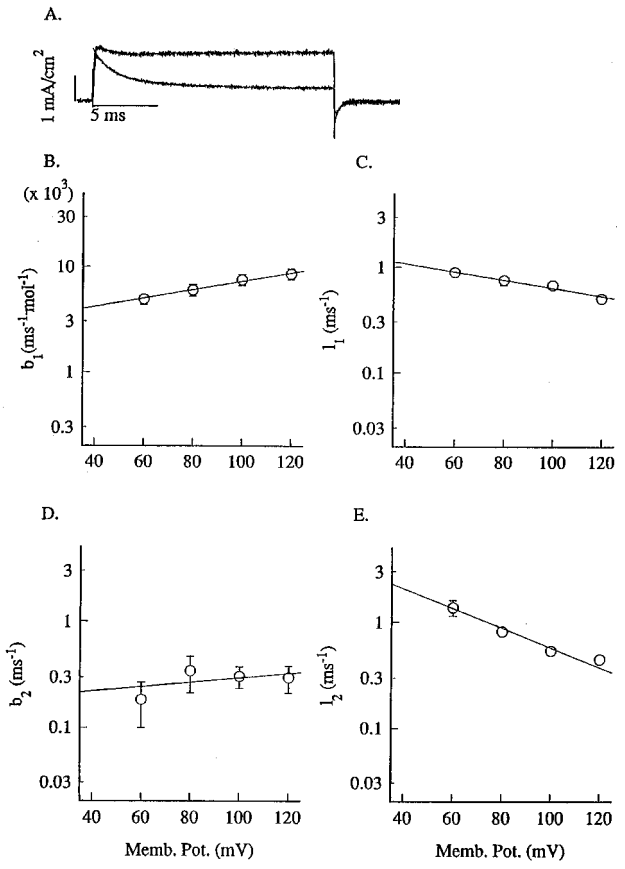

Figure 4 Time course of G-cyclam induced inhibition of I_{Na} in pronase-treated axon. (A) Original I_{Na} traces in 50 Na^+-ASW/50 Na^+-SIS medium. The falling phase of I_{Na} in 3×10^{-5} M G-cyclam is well fitted with the sum of two exponential functions and the fitted curve is superimposed on I_{Na} record. The fast time constant was estimated to be 0.99 ms and the slow time constant to be 3.88 ms by a least-square algorithm. (B) Relationship between the rate constants and the membrane potentials. The method for deriving the rate constants is based on the assumption that two sequential blocking steps occur in direct connection to the open state. The probability for the channel to be in the open state is expressed by the following equation:

$$P_{open}(t) = C_1 \cdot \exp(-\lambda_1 \cdot t) + C_2 \cdot \exp(-\lambda_2 \cdot t) + C_3 \quad (1)$$

where C_1, C_2, C_3, λ_1 and λ_2 are constants. All these parameters are obtained by fitting eq. (1) to the falling phase of I_{Na} in the presence of macrocyclic polyamine analogs. If one assumes that the channel is in the fully open state at the beginning of stimulating pulses, $C_1 + C_2 + C_3 = 1$ and each rate constant for this molecule is expressed as follows:

$$b_1 = k_1/[\text{G-cyclam}] = (\lambda_1 \cdot C_1 + \lambda_2 \cdot C_2)/[\text{G-cyclam}]$$

$$l_1 = \lambda_2 - \lambda_1 \cdot C_1 - \lambda_2 \cdot C_2 + C_1 \cdot \lambda_1 \cdot (\lambda_1 - \lambda_2)/(\lambda_1 \cdot C_1 + \lambda_2 \cdot C_2)$$

$$b_2 = \lambda_1 - \lambda_2 - C_1 \cdot \lambda_1 \cdot (\lambda_1 - \lambda_2)/(\lambda_1 \cdot C_1 + \lambda_2 \cdot C_2)$$

$$l_2 = C_3 \cdot \lambda_1 \cdot \lambda_2/(\lambda_2 - \lambda_1 \cdot C_1 - \lambda_2 \cdot C_2 + C_1 \cdot \lambda_1 \cdot (\lambda_1 - \lambda_2)/$$
$$(\lambda_1 \cdot C_1 + \lambda_2 \cdot C_2)),$$

where b_1 and l_1 are on- and off-rate constants for the first blocking stage and b_2 and l_2 those for the second blocking stage. Straight lines are drawn by $b_1 = 2.87 \times 10^3 \cdot \exp(0.0091 \cdot E)$, $l_1 = 1.583 \cdot \exp(-0.0092 \cdot E)$, $b_2 = 0.237 \cdot \exp(0.0026 \cdot E)$ and $l_2 = 4.67 \cdot \exp(-0.021 \cdot E)$ where E denotes the membrane potential in mV.

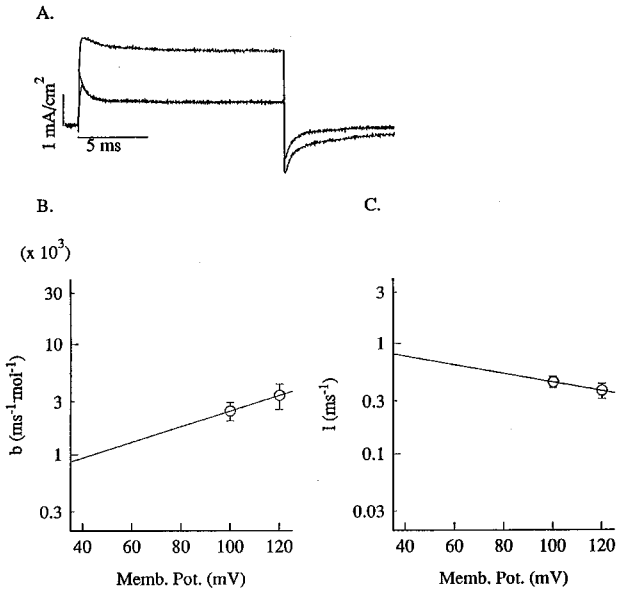

Figure 5 Time course of cyclam induced inhibition of I_{Na} in pronase-treated axon. (A) Original I_{Na} traces in 50 Na^+-ASW/50 Na^+-SIS medium. The falling phase of I_{Na} in 3×10^{-4} M cyclam is fitted with a single exponential function and the fitted curve is superimposed on I_{Na} records. The time constant was estimated to be 0.53 ms. (B) Relation between the rate constants and the membrane potential. The method for obtaining the rate constants is essentially the same as that in Figure 4, assuming $b_2=0$ and $C_2=0$ because the falling phase of I_{Na} is well fitted with a single exponential function. Straight lines are drawn by $b=487\cdot\exp(0.016\cdot E)$ and $l=1.10\cdot\exp(-0.0091\cdot E)$ where E denotes the membrane potential in mV.

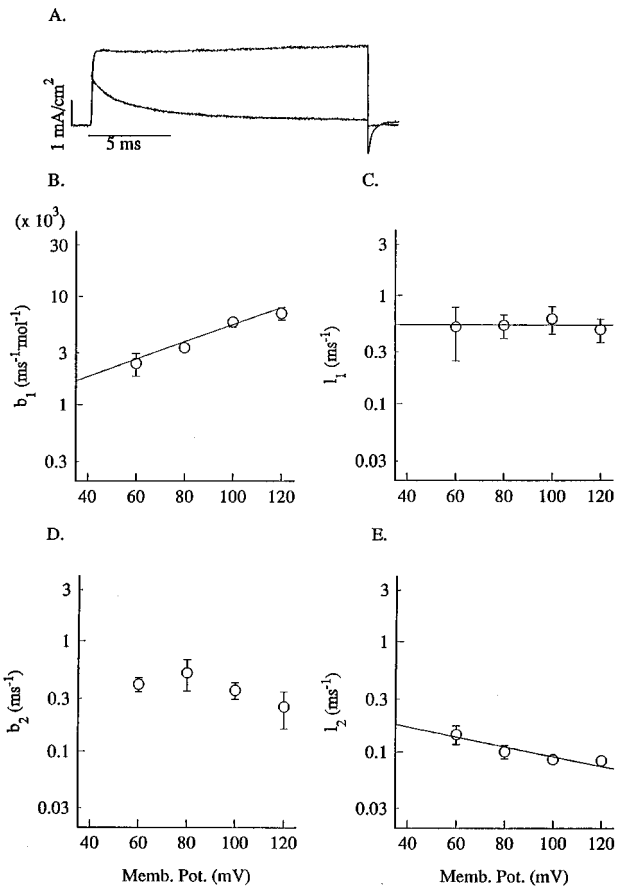

Figure 6 Time course of N4 induced inhibition of I_{Na} in pronase-treated axon. (A) Original I_{Na} traces in 50 Na^+-ASW/50 Na^+-SIS medium. The falling phase of I_{Na} in 1×10^{-4} M N4 is well fitted with the sum of two exponential functions, and the fitted curve is superimposed on I_{Na} record. The fast time constant was estimated to be 1.29 ms and the slow time constant to be 5.87 ms. (B) Relation between the rate constants and the membrane potentials. The method for obtaining the rate constants is essentially the same as that in Figure 4. A noteworthy point is that the tail current practically disappeared, as shown in (A). Straight lines are drawn by $b_1=911\cdot\exp(0.017\cdot E)$, $l_1=0.541\cdot\exp(-0.00014\cdot E)$, and $l_2=0.258\cdot\exp(-0.010\cdot E)$. In extrapolating the data for the rate constants to the membrane potential for -80 mV, the time constants are calculated to be 0.6 ms for the fast and 4 ms for the slow reaction, respectively. E denotes the membrane potential in mV.

and is plotted against the membrane potential of the test pulse (Figure 8A-2, B-2 and C-2).

Simulation of the block of Na^+ channel by G-cyclam

An *a priori* assumption that G-cyclam blocks Na^+ channels only in an open state, and the block and inactivation of Na^+ channels are mutually exclusive was examined by both experimental and simulation methods. The assumption predicts that, in the presence of the drug, during conditioning depolarization to +120 mV a certain proportion of Na^+ channels become nonconductive not only due to inactivation but also to block. Consequently, the proportion of Na^+ channels inactivated becomes smaller than under control conditions. Upon repolarization to −80 mV for 1 ms, the number of Na^+ channels available for ion permeation will become larger than that in control, because conductive Na^+ channels are supplied from those in the blocked state, as well as from those remaining in non-inactivated state, during conditioning pulses. For 1 ms repolarization, a fraction recovered from inactivation is estimated to be 18, and 92.5% of bound G-cyclam is calculated to be released. When the membrane is subjected to a test pulse to 0 mV for quantifying available Na^+ channels immediately after a short repolarization, more current is observed than that in control (Figure 9A). Figure 9B obtained from the simulation is qualitatively consistent with the experimental data shown in Figure 9A. Thus, it appears that G-cyclam blocks Na^+ channel in the open state and the resultant Na^+ channel in the blocked state does not change to an inactivated state.

Effect of internal solution pH on Na^+ channels block

Cyclic polyamine analogues do not change their conformation or charge distribution within the internal pH range of 6.1 to 8.5, over which the axonal activity can be preserved well (Kendig, 1981; Crumb & Clarkson, 1995). Thus, most changes in blocking action observed by fluctuating pH within this range can be attributed to conformational changes in Na^+ channels. The relation of K_D with the membrane potential for cyclam and G-cyclam remained unchanged (data not shown). Because pK_a is 7 and 10 for primary and secondary amine groups and pK_a is 12 for the terminal guanidyl group in NSTX-3, and the pK_a is 10 for primary and secondary amine groups in JSTX-3, NSTX-3 is more

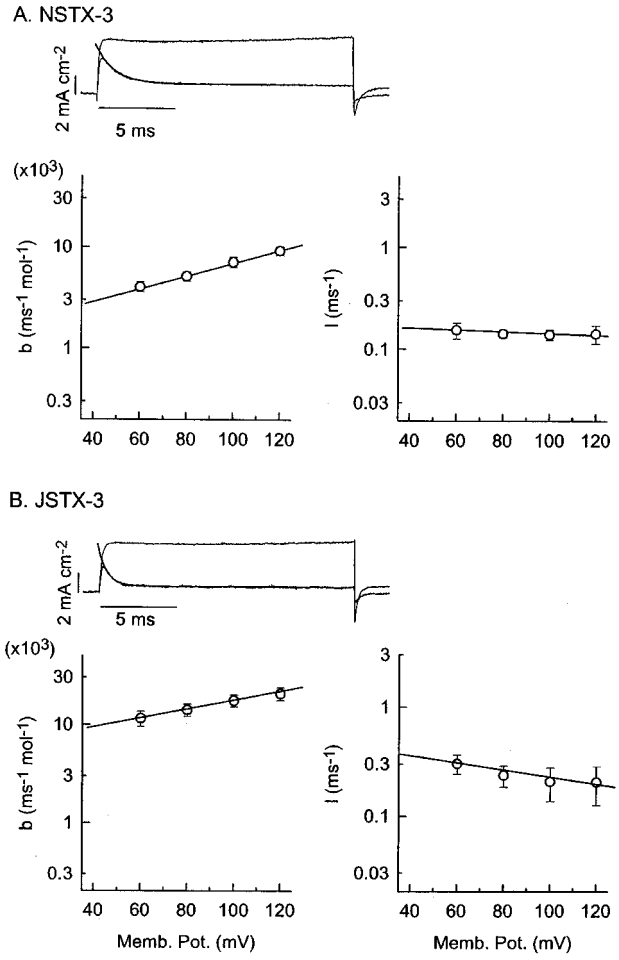

Figure 7 Time course of spider toxins induced inhibition of I_{Na} in pronase-treated axon. Original I_{Na} traces in 50 Na^+-ASW/50 Na^+-SIS medium and the relationship between the rate constants and the membrane potentials are shown. (A) NSTX-3. The falling phase of I_{Na} in 1×10^{-4} M NSTX-3 is well fitted with a single exponential function and the fitted curve is superimposed on I_{Na} records. The time constant was estimated to be 1.21 ms. The left-hand graph is for the binding constant and the right-hand graph for unbinding constant. The straight line for b is drawn by the equation of $b=1734\cdot\exp(0.0140\cdot E)$ and that for 1 by the equation of $1=0.164\cdot\exp(-0.0014\cdot E)$. All data were collected from a series of three experiments. The vertical bars are standard deviation of means. (B) JSTX-3. The falling phase of I_{Na} in 1×10^{-4} M JSTX-3 is well fitted with a single exponential function and the fitted curve is superimposed on I_{Na} records. The time constant was estimated to be 0.60 ms. The arrangement of the graph is the same as in (A). The straight lines for b and 1 are drawn by the equation of $b=6608\cdot\exp(0.00956\cdot E)$ and $1=0.441\cdot\exp(-0.00693\cdot E)$, respectively. E denotes the membrane potential in mV. All data were collected from a series of five experiments. The vertical bars have the same meaning as above.

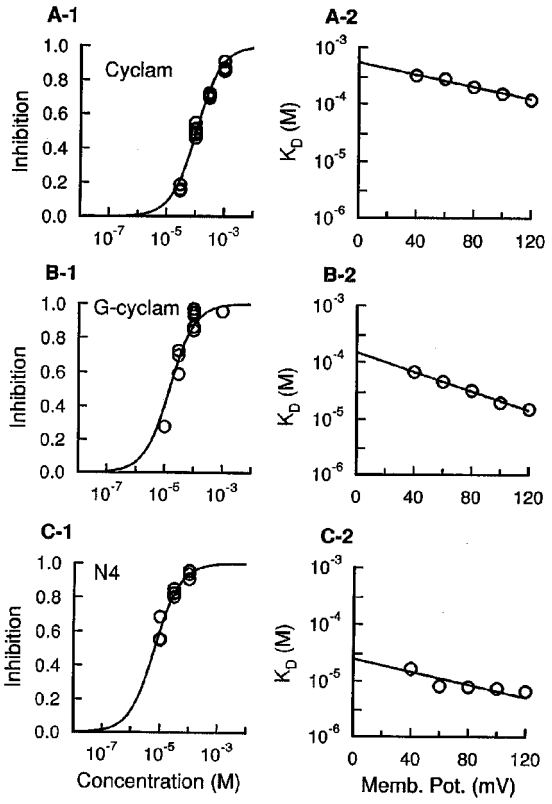

Figure 8 Voltage-dependent block of Na^+ channel. Relationship between relative inhibition of I_{Na} and concentrations of drug is illustrated in A-1 for cyclam, in B-1 for G-cyclam and C-1 for N4. In the case of N4, because I_{Na} did not reach the steady state at the end of a 14 ms pulse (e.g. Figure 6A), the estimation of I_{Na} was carried out with fitting the exponential curve to data. Smooth lines are drawn assuming one-to-one stoichiometry. The half maximum concentrations for cyclam, G-cyclam and N4 are plotted against the membrane potential of test pulse in A-2, B-2 and B-3, respectively. Straight lines are drawn by $K_D(E)=5.42\times10^{-4}\cdot\exp(-0.012\cdot E)$ in A-2, $1.48\times10^{-4}\cdot\exp(-0.019\cdot E)$ in B-2, and $2.47\times10^{-5}\cdot\exp(-0.013\cdot E)$ in C-2, respectively. E denotes the membrane potential in mV. All data were collected in 50 Na^+-ASW/50 Na^+-SIS.

protonated at internal pH = 6.1 than it is at pH = 7.3. The finding that a drastic enhancement of blocking capability for NSTX-3 occurred at pH 6.1 (Figure 10) is most likely due to an increase in the number of positive charges of this molecule.

Effect of G-cyclam on the gating currents of I_{Na}

The results obtained so far indicate that all these chemicals plug Na^+ channels in the open state. Since the movement of the gating charge when channels close is hindered by the inactivation particles attached to the channel mouth (Armstrong, 1981), the gating current after the pulse ($I_{g,off}$) is thought to be more susceptible to the action of drug than the gating current on applying depolarizing pulse ($I_{g,on}$). Figure 11A shows that was the case. In intact axons, $I_{g,on}$ remained unchanged before and after the administration of drugs. However, G-cyclam not only trims the peak of $I_{g,off}$, but also slows down its rate of decay (Tables 2 and 3). The total charges of $I_{g,off}$ tended to increase (Figure 11A and Table 2). Suppression of $I_{g,off}$ was also observed in the pronase-treated axons (Figure 11B and Table 2), implying that G-cyclam can enter the internal mouth of a Na^+ channel during its opening, and that bound G-cyclam hampers the movement of the intramembraneous charged particle. Moreover, it needs about a 1 ms for the drugs to be released almost completely from the receptor site, even though this is a quick response. Thus, the time course of $I_{g,off}$ is prolonged, compared with that of $I_{g,off}$ in control. The total charges moved during the off process of the activation gate remained unchanged in pronase-treated axons (Table 2). Change in the

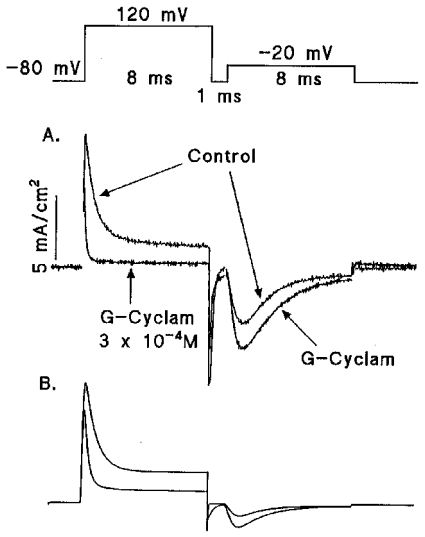

Figure 9 Experimental confirmation of the anticipation inferred from experimental data for rate constants. (A) Change in I_{Na} in the absence and presence of G-cyclam in response to the protocol shown above. (B) Simulation of the behaviour of I_{Na}. The main parameters for I_{Na} were taken from Hodgkin & Huxley (1952) after a temperature correction. During +120 mV depolarizing pulse, α_h of 0.255 ms^{-1} and β_h of 1.179 ms^{-1} were obtained from the single exponential curve adopted to the falling phase of I_{Na} in (A). The rate constants necessary for the simulation experiment were calculated from the four equations for b_1, b_2, l_1 and l_2 in 50 Na^+-ASW/50 Na^+-SIS shown in Figure 4. The calculated values of b_1 are 8553, 1386 and 2392 ms^{-1} mol^{-1} for +120 mV, −80 mV and −20 mV, those of b_2 0.322, 0.193, 0.225 ms^{-1}, those of l_1 0.527, 3.296, 1.902 ms^{-1} and those of l_2 0.374, 25.12 and 7.11 ms^{-1}, respectively. E denotes the membrane potential in mV.

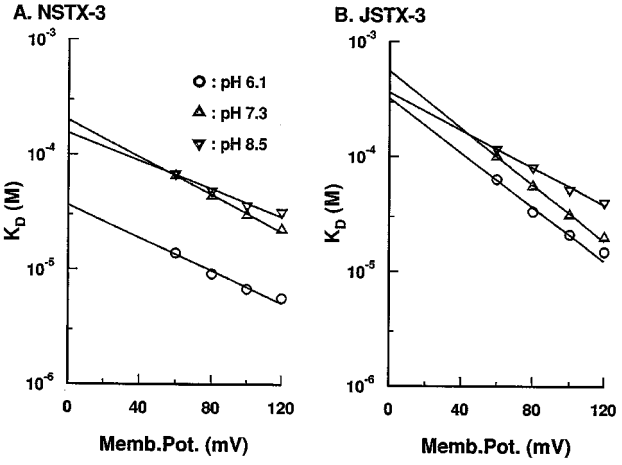

Figure 10 Dependence of K_D for the spider toxins on the membrane potential and internal pH. The values of K_D of each toxin were estimated as shown in Figure 8 at several membrane potentials. Each data point was collected from the experiments done on three axons. Straight lines in (A) are drawn by $K_D(E) = 1.54 \times 10^{-4} \cdot \exp(-0.0140 \cdot E)$ for pH = 8.5, $2.00 \times 10^{-4} \cdot \exp(-0.0187 \cdot E)$ for pH = 7.3 and $3.65 \times 10^{-5} \cdot \exp(-0.0164 \cdot E)$ for pH = 6.1. Those in (B) were drawn by the equation of $K_D(E) = 3.61 \times 10^{-4} \cdot \exp(-0.0188 \cdot E)$ for pH = 8.5, $5.56 \times 10^{-4} \cdot \exp(-0.0285 \cdot E)$ for pH = 7.3 and $3.27 \times 10^{-4} \cdot \exp(-0.0273 \cdot E)$ for pH = 6.1. E denotes the membrane potential in mV.

time constants for $I_{g,off}$ in both intact and pronase-treated axons is listed in Table 3.

Discussion

The results obtained in this study concerning the effect of three cyclic polyamine derivatives and two spider toxins on Na^+ channel in squid axon is summarized as follows: (1) these compounds solely exert a blocking action on Na^+ channel from the internal phase when Na^+ channels open; (2) their blocking effect is voltage-dependent, in such a way that the more the membrane depolarizes, the more prominent is the suppression; (3) the tail current in intact axon generated on the termination of a square pulse is prolonged as well as increased in the presence of G-cyclam and cyclam; (4) G-cyclam and cyclam do not affect $I_{g,on}$ but suppress peak $I_{g,off}$, followed by a prolongation of the time course of the falling phase.

For the sake of brevity, we will use the simplest kinetic model for simulating Na^+ channel behaviour in the presence of these drugs. It is assumed that drugs enter Na^+ channels pores only when the channels open, and once drugs bind to channels, channels are trapped in a blocked state and cannot shift to an inactivated state. Using the double pulse protocol, one can experimentally test this assumption by showing whether or not I_{Na} generated by the second test pulse becomes bigger in the presence of drug (relative to control), provided that the membrane repolarizes to the holding potential of −80 mV for a short time in order to relieve Na^+ channels from the blocked state. As shown in Figure 9, that was the case. The change in gating current induced by G-cyclam supports the hypothesis that the drugs only bind to channels in open state. Because these drugs interact with Na^+ channels only in open state, $I_{g,off}$ was suppressed by them, while $I_{g,on}$ remained unchanged, regardless of the presence or absence of inactivation process. Because the rate constant for releasing these drugs from the binding site is large, compared with that for the movement of inactivation particles, gating particles that have been immobilized by the drugs in intact axons become free to move as the drugs detach from the binding sites, yielding $I_{g,off}$ with a slowly decaying time course (Tables 2 and 3). In pronase-treated axons, $I_{g,off}$ is solely due to the movement of intramembraneous charged particles after drugs quickly detach from the binding sites. Therefore, the total charge movement of $I_{g,off}$ before and after the application of drug was equal (Table 2), as Yeh & Armstrong (1978) had anticipated. However, in intact axon, an immobilized fraction of the gating charge by inactivation particles in the presence of drugs is less than that in control because a certain proportion of Na channels are blocked by the drug and inactivation particles cannot bind to these blocked Na^+ channels. Thus, off-gating charge from blocked Na^+ channels finally contribute to the increase in the total charge movement of $I_{g,off}$, as drugs dissociate from the channels, compared with unblocked but normally inactivated Na^+ channels. As shown in Figure 11, a small increase in the integrated value of $I_{g,off}$ was actually observed in six out of nine experiments. Armstrong & Bezanilla (1974; 1977) observed a similar phenomenon in intact axon by repolarizing the membrane to the very negative membrane potential of −140 mV, because this accelerates the detachment of

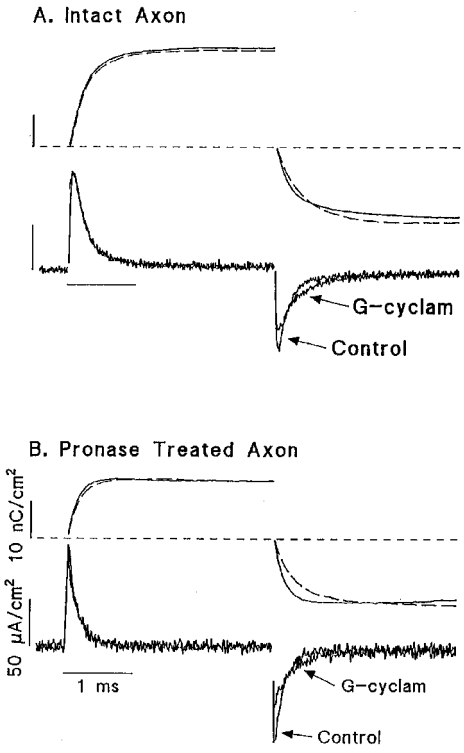

Figure 11 Inhibition of gating current by G-cyclam. I_g was recorded in Na-free ASW/Na-free SIS. The P-P/4 method (Armstrong & Bezanilla, 1974) was used with a P/4 pulse starting from the potential of −150 mV. Average currents for the four trials are shown. The lower graph in (A) shows the reduction in $I_{g,off}$ in intact axon by 1×10^{-3} M G-cyclam. The $I_{g,off}$ was recorded on return to −80 mV after the membrane was held at +10 mV for 3 ms. The upper graph in (A) shows the total charge movement of gating currents. The total charge during turn-on or turn-off was determined by integrating the gating current as a function of time. Zero current level was determined by averaging the points from 2.5 to 3 ms after either an on or off step pulse was given. The resultant charge movement for control is presented with the solid line, and that for G-cyclam the dotted line (upper graph). Corresponding original records are shown in the lower portion. In (B), all records were collected using the same protocol as those in (A) on pronase-treated axon. The calibration bars in (B) are also applicable to those in (A).

Table 2 Relative values for total charge movement (Q) and peak of $I_{g,off}$

	$\frac{Q_{on}^*}{Q_{on}}$	$\frac{Q_{off}}{Q_{on}}$	$\frac{Q_{off}^*}{Q_{on}}$	$\frac{Peak^*}{Peak}$	n
Intact axon					
G-cyclam	1.03±0.06	0.81±0.05	0.85±0.08	0.74±0.06	9
Cyclam	1.01±0.03	0.78±0.11	0.83±0.07	0.79±0.05	9
Pronase axon					
G-cyclam	0.97±0.06	1.01±0.07	1.01±0.04	0.77±0.09	6
Cyclam	0.96±0.05	1.01±0.06	0.99±0.10	0.80±0.13	6

Q_{on}: Total charge movement during $I_{g,on}$. Q_{off}: Total charge movement during $I_{g,off}$. Asterisks (*) denote data in the presence of drugs.

inactivation particles. Yeh & Armstrong (1978) have observed that the internal introduction of pancuronium into axons of which inactivation process had been removed with pronase-treatment can restore a decay phase of $I_{g,off}$ resembling the gating current immobilization in normal axon, and they suggested that inactivation apparatus might

Table 3 Time constants for $I_{g,off}$

	τ_{fast} (ms)	τ_{slow} (ms)	n
Intact axon			
Control	0.12±0.03	1.15±0.12	9
G-cyclam	0.17±0.04*	0.96±0.34	
Control	0.11±0.02	1.00±0.28	9
Cyclam	0.15±0.03*	0.97±0.28	
Pronase axon			
Control	0.26±0.07		6
G-cyclam	0.36±0.06*		
Control	0.30±0.05		6
Cyclam	0.37±0.03*		

*$P<0.05$ from control.

compete with the binding site common to pancuronium. Recent fluorescence and point mutation studies have revealed that the domain IV S4-S5 linker interacts with IFM motif in the linker between domain III and IV (McPhee *et al*., 1998) and that the S4 in domains III and IV are responsible for the linkage of voltage sensor with fast inactivation (Cha *et al*., 1999). Furthermore, Sheets *et al*. (2000) have suggested that S4 in domain III contributes to charge immobilization only after binding of the inactivation particle. Taking into account all these considerations, it is reasonable to speculate that the change in $I_{g,off}$ is likely due to binding of these drugs to the sites where inactivation particles normally bind.

Blocking effect may be influenced by the positive charges and hydrophobicity arising from the following common structures among the drugs used in this study. Cyclam, G-cyclam and N-4 each consist of a macrocyclic polyamine ring, and G-cyclam and N-4 have in addition a side chain of a alkylguanidinium and 2,4-dihydroxyphenylacethylasparaginyl cadaverine (DAAC) group, respectively. JSTX-3 and NSTX-3 consist of DAAC group in common and the side chains of spermidine and argynylaminobutylamine, respectively. As to the positive charge, the macrocyclic polyamine ring retains two positive charges at the pH explored, because the ring consists of four amine groups, the pK_as of which are 2, 2, 10 and 11. G-cyclam carries an additional positive charge on the guanidyl group. The spermidine group in JSTX-3 holds a positive charge on each of three amine groups all with pK_as of 10. At the pH range studied in this experiment, the charges on JSTX-3 remain unchanged. On the other hand, NSTX-3 has two positive charges on the secondary amine and terminal guanidinium group in which the value of pK_a is 10 and 12, respectively. Because the primary amine sitting inbetween has pK_a=7, this amine bears a positive charge, when internal pH changes from 7.3 to 6.1. The remaining DAAC part does not carry an electrical charge. Another molecular characteristic of these compounds is hydrophobicity. Macrocyclic polyamines can also be accommodated into a hydrophobic environment by hiding the hydrogen groups in the centre of the macrocyclic polyamine ring (Nave & Truter, 1974). Both JSTX-3 and NSTX-3 may be able to take a circular conformation in aqueous medium by hydrogen bonding between the secondary amine and amide groups and the resultant configurations are also similar to the macrocyclic

polyamine. Since the DAAC group retains a hydrophobic property and the macrocyclic polyamine ring can take a reversible conformation adaptable to a hydrophobic environment, all the chemicals examined may be considered to be at least partly hydrophobic.

An experiment was conducted by changing the internal pH, differentiating two possibilities for the blocking action, the presence of positive charge and the molecular hydrophobicity. At the pH range explored, NSTX-3 is the sole molecule with enhanced blocking action when the internal pH is changed from 7.3 to 6.1. Because the protonation of the amines in NSTX-3 increases from 2 to 3, it is reasonable to think that the primary factor in enhancing blocking potency is the increase of positive charge. By comparing the results shown in Figure 8A-2 with those in B-2, it can be seen that the increase in the positive charge also enhances potency. The hydrophobicity factor is also influential. For example, as shown in Figure 8A-2 and C-2, the blocking action is enhanced as the side chain becomes hydrophobic. Another noticeable finding related to the hydrophobic moiety in the molecule is that the binding and unbinding process becomes slower when the hydrophobic DAAC group is introduced. In connection with this finding, in a medium containing N4 and spider toxins, tail currents after a pulse substantially decreased (Figure 6), implying that the reaction for the transition from the blocked to open states may proceed so slowly that current flown through the small fraction of unblocked Na^+ channels resolves into noise.

Additional hydrophobic pathways for the drugs such as local anaesthetics to access the binding site may enhance the blocking action as described by Courtney (1975) or Hille (1977). However, it is not the case for the drugs studied here, because it is thought that they can only access the channel in its open state, and the drugs used in this study are not entirely hydrophobic. Hydrophobicity of these drugs could act differently, for example by stabilizing drug-bound conformation of the channel.

In summary, the requirements for molecules to block Na^+ channels from the internal phase in this study are (1) positive charges, where the distribution is more decisive than the total number, and (2) hydrophobicity is an important factor in intensifying the blocking capability and slowing the rate constants of the binding and unbinding processes of drugs.

This work was supported by research grants from the ministry of Education, Science and Culture, Japan, and the Uehara foundation.

References

ARAMAKI, Y., YASUHARA, T., HIGASHIJIMA, T., YOSHIOKA, M., MIWA, A., KAWAI, N. & NAKAJIMA, T. (1986). Chemical characterization of spider toxin, JSTX and NSTX. *Proc. Jpn. Acad. Ser. B.,* **62,** 359 – 362.

ARMSTRONG, C.M. (1969). Inactivation of the potassium conductance and related phenomena caused by quaternary ammonium ion injection in squid axons. *J. Gen. Physiol.,* **54,** 553 – 575.

ARMSTRONG, C.M. (1981). Sodium channels and gating currents. *Physiol. Rev.,* **61,** 644 – 683.

ARMSTRONG, C.M. & BEZANILLA, F. (1974). Charge movement associated with the opening and closing of the activation gates of the Na channels. *J. Gen. Physiol.,* **63,** 533 – 552.

ARMSTRONG, C.M. & BEZANILLA, F. (1977). Inactivation of the sodium channel. II. Gating current experiments. *J. Gen. Physiol.,* **70,** 567 – 590.

ARMSTRONG, C.M. & CROOP, R.S. (1982). Simulation of Na channel inactivation by thiazine dyes. *J. Gen. Physiol.,* **80,** 641 – 662.

CAHALAN, M.D. & ALMERS, W. (1979). Block of sodium conductance and gating current in squid giant axons poisoned with quaternary strychnine. *Biophys. J.,* **27,** 57 – 73.

CHA, A., RUBEN, P.C., GEORGE JR., A.L., FUJIMOTO, E. & BEZANILLA, F. (1999). Voltage sensors in domain III and IV, but not I and II, are immobilized by Na^+ channel fast inactivation. *Neuron,* **22,** 73 – 87.

CHANDLER, W.K. & MEVES, H. (1970). Sodium and potassium currents in squid axons perfused with fluoride solutions. *J. Physiol. (Lond.),* **211,** 623 – 652.

COURTNEY, K.R. (1975). Mechanism of frequency-dependent inhibition of sodium currents in frog myelinated nerve by the lidocaine derivative GEA 968. *J. Pharmacol. Exp. Ther.,* **195,** 225 – 236.

CRUMB JR., W.J. & CLARKSON, C.W. (1995). The pH dependence of cocain interaction with cardiac sodium channels. *J. Pharmacol. Exp. Ther.,* **274,** 1228 – 1237.

FOZZARD, H.A. & HANCK, D.A. (1996). Structure and function of voltage-dependent sodium channels: comparison of brain II and cardiac isoforms. *Physiol. Rev.,* **76,** 887 – 926.

HILLE, B. (1977). Local anesthetics: Hydrophilic and hydrophobic pathways from the drug-receptor reaction. *J. Gen. Physiol.,* **69,** 497 – 515.

HODGKIN, A.L. & HUXLEY, A.F. (1952). A quantitative description of membrane current and its application to conduction and excitation in nerve. *J. Physiol. (Lond.),* **117,** 500 – 544.

KAWAI, N., MIWA, A., HASHIMOTO, Y., SHUDO, K., ASAMI, T. & NAKAJIMA, T. (1989). Zinc ion enhances the blocking potency of synthetic analogs of spider toxin (JSTX) on the glutamate receptor. *Neurosci. Res.,* **6,** 358 – 362.

KENDIG, J.J. (1981). Barbiturates: active form and site of action at node of Ranvier sodium channels. *J. Pharmacol. Exp. Ther.,* **218,** 175 – 181.

MCPHEE, J.C., RAGSDALE, D.S., SCHEUER, T. & CATTERALL, W.A. (1998). A critical role for the S4-S5 intracellular loop in domain IV of the sodium channel alpha-subunit in fast inactivation. *J. Biol. Chem.,* **273,** 1121 – 1129.

NARAHASHI, T. & ANDERSON, N.C. (1967). Mechanism of excitation block by the insecticide allethrin applied externally and internally to squid giant axons. *Toxicol. Appl. Pharmacol.,* **10,** 529 – 547.

NAVE, C. & TRUTER, M.R. (1974). Crystal structure of the dihydroperchlorate of 1,4,8,11-tetra-azacyclotetradecane (Cyclam). *J. Chem. Soc. Dalton Trans.,* 2351 – 2354.

NODA, M., SHIMIZU, S., TANABE, T., TAKAI, T., KAYANO, T., IKEDA, T., TAKAHASHI, H., NAKAYAMA, H., KANAOKA, Y., MINAMINO, N., KANGAWA, K., MATSUO, H., RAFTERY, M.A., HIROSE, T., INAYAMA, S., HAYASHI, H., MIYATA, T. & NUMA, S. (1984). Primary structure of Electrophorus electricus sodium channels deduced from cDNA sequence. *Nature,* **312,** 121 – 127.

ROGERS, J.C., QU, Y., TANADA, T.N., SCHEUER, T. & CATTERALL, W.A. (1996). Molecular determinants of high affinity binding of α-scorpion toxin and sea anemone toxin in the S3-S4 extracellular loop in domain IV of the Na^+ channel α subunit. *J. Biol. Chem.,* **271,** 15950 – 15962.

ROJAS, E. & RUDY, B. (1976). Destruction of the sodium conductance inactivation by a specific protease in perfused nerve fibres from Loligo. *J. Physiol. (Lond.),* **262,** 501 – 531.

SHEETS, M.F., KYLE, J.W. & HANCK, D.A. (2000). The role of the putative inactivation lid in sodium channel gating current immobilization. *J. Gen. Physiol.,* **115,** 609 – 620.

WU, C.H. & NARAHASHI, T. (1973). Mechanism of action of propranolol on squid axon membranes. *J. Pharmacol. Exp. Ther.,* **184,** 155 – 162.

YEH, J.Z. & ARMSTRONG, C.M. (1978). Immobilization of gating charge by a substance that simulates inactivation. *Nature,* **273,** 387 – 389.

YEH, J.Z. & NARAHASHI, T. (1977). Kinetic analysis of pancuronium interaction with sodium channels in squid axon membranes. *J. Gen. Physiol.,* **69,** 293 – 323.

(Received May 30, 2000
Revised September 4, 2000
Accepted October 12, 2000)